ELSEVIER

Journal of Biomechanics 40 (2007) 2636–2644

JOURNAL OF BIOMECHANICS

www.elsevier.com/locate/jbiomech
www.JBiomech.com

Learning to walk with a robotic ankle exoskeleton

Keith E. Gordon[a,*], Daniel P. Ferris[a,b,c]

[a]Division of Kinesiology, University of Michigan, 401 Washtenaw Avenue, Ann Arbor, MI 48109-2214, USA
[b]Department of Biomedical Engineering, University of Michigan, 401 Washtenaw Avenue, Ann Arbor, MI 48109-2214, USA
[c]Department of Physical Medicine and Rehabilitation, University of Michigan, 401 Washtenaw Avenue, Ann Arbor, MI 48109-2214, USA

Accepted 5 December 2006

Abstract

We used a lower limb robotic exoskeleton controlled by the wearer's muscle activity to study human locomotor adaptation to disrupted muscular coordination. Ten healthy subjects walked while wearing a pneumatically powered ankle exoskeleton on one limb that effectively increased plantar flexor strength of the soleus muscle. Soleus electromyography amplitude controlled plantar flexion assistance from the exoskeleton in real time. We hypothesized that subjects' gait kinematics would be initially distorted by the added exoskeleton power, but that subjects would reduce soleus muscle recruitment with practice to return to gait kinematics more similar to normal. We also examined the ability of subjects to recall their adapted motor pattern for exoskeleton walking by testing subjects on two separate sessions, 3 days apart. The mechanical power added by the exoskeleton greatly perturbed ankle joint movements at first, causing subjects to walk with significantly increased plantar flexion during stance. With practice, subjects reduced soleus recruitment by ~35% and learned to use the exoskeleton to perform almost exclusively positive work about the ankle. Subjects demonstrated the ability to retain the adapted locomotor pattern between testing sessions as evidenced by similar muscle activity, kinematic and kinetic patterns between the end of the first test day and the beginning of the second. These results demonstrate that robotic exoskeletons controlled by muscle activity could be useful tools for testing neural mechanisms of human locomotor adaptation.

Keywords: Gait; Motor learning; Biomechanics; Powered orthosis; Locomotion; EMG

1. Introduction

Motor adaptation is critical for successful locomotion. Humans regularly modulate muscle activity during walking in response to environmental (e.g. terrain, obstacles) and neuromuscular (e.g. fatigue, muscle strength) factors. While many studies have examined human locomotor adaptation to environmental perturbations (Tokuhiro et al., 1985; Ferris and Farley, 1997; Farley et al., 1998; Ferris et al., 1998; Leroux et al., 1999; Prentice et al., 2004; Marigold and Patla, 2005; Lay et al., 2006; Maclellan and Patla, 2006), it has been more difficult to study human locomotor adaptation to controlled neuromuscular perturbations. Researchers have studied neuromuscular locomotor adaptation in animal models using botulinum toxin, nerve transections, and spinal cord lesions (Lam and Pearson, 2002). However, the invasiveness of these procedures make them unsuitable for comparable human studies.

There is a critical need to understand how humans adapt locomotor control in response to alterations in neuromuscular dynamics. Neurological insult, such as stroke, and spinal cord injury, leads to discoordinated locomotion and requires motor adaptation to restore mobility (Grasso et al., 2004; Kautz and Brown, 1998). From a clinical perspective, it is imperative to identify principles governing locomotor adaptation to perturbations disrupting muscular coordination.

We developed a novel robotic perturbation to study human locomotor adaptation to disrupted muscle coordination. The perturbation is a pneumatically powered ankle exoskeleton (Ferris et al., 2005, 2006; Sawicki et al., 2006). The exoskeleton has a hinged ankle joint and an artificial

*Corresponding author. Rehabilitation Institute of Chicago, 345 E. superior St., Rm. 1406, Chicago, IL 60611, USA. Tel.: +1 312 238 2996; fax: +1 312 238 2208.
E-mail address: keith-gordon@northwestern.edu (K.E. Gordon).

0021-9290/$ - see front matter © 2007 Elsevier Ltd. All rights reserved.
doi:10.1016/j.jbiomech.2006.12.006

pneumatic muscle providing plantar flexor torque (Fig. 1). We focused on the ankle joint because it produces more mechanical power during walking than either the hip or knee joint (Meinders et al., 1998) and is a major factor limiting mobility after neurological injury (Nadeau et al., 1999; Kim and Eng, 2003; Kim et al., 2004).

In this study, the exoskeleton was proportionally activated by the user's soleus electromyography (EMG), effectively increasing soleus muscle strength. We examined neurologically intact subjects walking with the exoskeleton on two separate days. We hypothesized that gait would be initially distorted by the exoskeleton, but that the effect would decrease with practice due to a reduction in soleus muscle recruitment. By testing subjects on two separate days, we were able to examine whether subjects stored a walking motor pattern that reflected exoskeleton dynamics.

2. Methods

Ten healthy subjects (5 male, 5 female, mean ± SD, age 25.8 ± 2.3 years and mass 75.3 ± 12.2 kg) gave written informed consent and participated in the study. The University of Michigan Medical School Institutional Review Board approved the protocol.

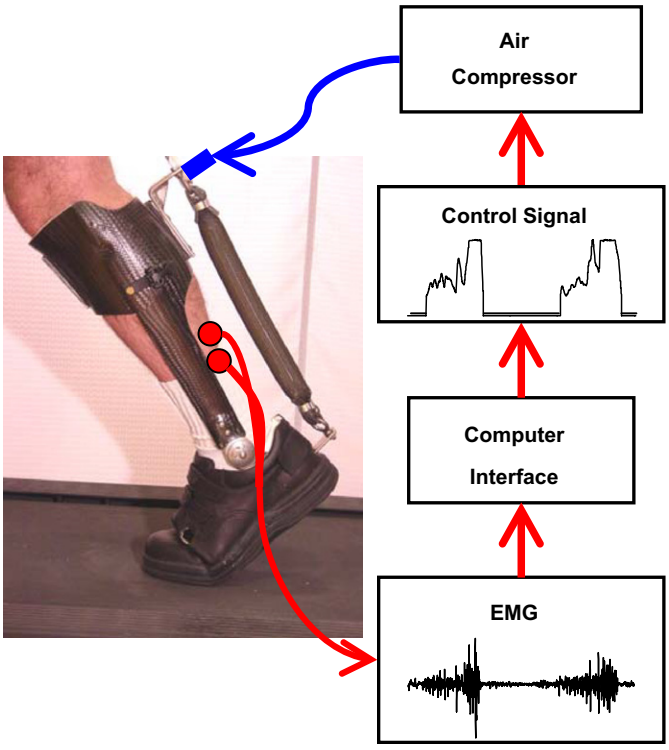

Fig. 1. Subjects wore a custom fit exoskeleton on their left lower limb. The exoskeleton was hinged at the ankle to allow unimpeded sagittal plane rotation during walking. The exoskeletons had an average total weight of 1.2 ± 0.1 kg (mean ± SD) and moment arm length of 10.0 ± 1.0 cm (mean ± SD) that varied depending on the size of the subject. Electrodes placed on the skin of the subject's leg recorded electrical signals (EMG) of the soleus muscle. A computer processed the EMG to control air pressure in an artificial pneumatic muscle so that there was a proportional relationship between EMG and air pressure. As air pressure increases, it caused the artificial muscle to develop tension. The exoskeleton effectively increased ankle torque produced by soleus muscle activation.

We constructed a custom fit exoskeleton for the left lower limb of each subject (Fig. 1). Construction and testing of earlier prototypes of the exoskeleton have been described in detail (Ferris et al., 2005, 2006; Gordon et al., 2006). The exoskeleton consisted of a carbon fiber shank section and a polypropylene foot section. A metal hinge between the sections allowed free sagittal plane rotation of the ankle joint.

An artificial pneumatic muscle attached to the posterior of the exoskeleton provided plantar flexor torque. Increasing air pressure (0–6.2 bar) caused the artificial muscle to increase force. Air pressure regulators produced sounds that were audible to the subjects.

We implemented proportional myoelectric control of the artificial muscle through a desktop computer and real-time control board (dSPACE Inc.). Custom software regulated air pressure in the artificial muscle proportional to processed soleus EMG amplitude (Movie 1 online supplement). EMG signals from the soleus used to control the artificial muscle were high-pass filtered with a second-order Butterworth filter (cutoff frequency 20 Hz) to remove movement artifact, full wave rectified, and low-pass filtered with a second order Butterworth filter (cutoff frequency 10 Hz) to smooth the signal. Threshold cutoffs eliminated background noise. Adjustable gains scaled the control signals. During walking, artificial muscle force production is modulated by three primary factors: activation, muscle length and bandwidth (Gordon et al., 2006). There is no simple linear gain relating EMG amplitude to artificial muscle force. More details on artificial muscle and orthosis mechanics can be found in previous studies (Ferris et al., 2005, 2006; Gordon et al., 2006).

We recorded kinematic, kinetic, and electromyography data during the first 10 s of every minute while subjects walked on a treadmill at 1.25 m/s. We collected three-dimensional kinematics using a 6-camera video system (120 Hz, Motion Analysis Corporation, Santa Rosa, CA) and step-cycle data using footswitches. We collected artificial muscle force with a force transducer (1200 Hz, Omega Engineering). We recorded EMG (1200 Hz, Konigsberg Instruments Inc.,) from the left soleus, tibialis anterior, medial gastrocnemius, lateral gastrocnemius, vastus lateralis, vastus medialis, rectus femoris and medial hamstring muscles using bipolar surface electrodes. Before walking we inspected EMG during manual muscle tests and moved electrodes to minimize crosstalk. Electrode position was marked on each subject using permanent ink to guarantee consistent placement between sessions. While it is possible that subjects in this study would demonstrate locomotor adaptations in both lower limbs, we have selected to focus this study only on the changes occurring in the left (perturbed) limb.

Subjects completed two identical testing sessions 72 h apart. During each session, subjects walked for 10 min with the exoskeleton passive (baseline), then 30 min with the exoskeleton powered (powered), and finally 15 min with the exoskeleton passive (post-adaptation). Transitions between conditions were performed without stopping. We selected a 3-day period between sessions to allow sufficient time for motor consolidation to occur and to allow recovery from potential muscle soreness. Before testing, subjects were informed that the exoskeleton would "increase the strength of their soleus muscle", but they were not given any practice walking in the exoskeleton. Subjects were instructed to walk in the manner that they felt most comfortable without holding onto the treadmill. Subjects received no additional external feedback about ankle kinematics or kinetics.

We created average step-cycle profiles for EMG, kinematic and kinetic variables for each subject. Average step-cycle profiles were calculated from all complete step cycles recorded during each minute of walking (8–12 cycles). To examine changes in EMG amplitude, we calculated normalized root mean squared (RMS) EMG values for both stance and swing phases of the gait cycle. RMS values were calculated from EMG data that was high-pass filtered (cutoff frequency 20 Hz), rectified and normalized to the final minute of baseline on a given testing day. We also created step-cycle profiles for joint angles calculated from smoothed marker data (low-pass filtered, cutoff frequency 6 Hz). To examine changes in kinematics across time, we calculated ankle, knee and hip joint angle Pearson product moment correlations between average step-cycle joint angle profiles for each minute of walking versus average step-cycle joint angle profile during the final minute of baseline on a given testing day (Fig. 2). We used the

common variance of the correlation (r^2) to assess similarity between ankle joint patterns at the two instances in time. We also calculated average exoskeleton positive and negative mechanical work during the step cycle.

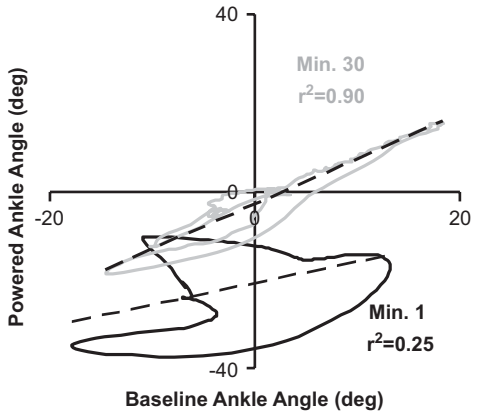

Fig. 2. Linear correlation between baseline and powered ankle joint kinematic patterns. Example data are plotted for one subject during the first minute of powered walking (minute 1) and the 30th minute of powered walking (minute 30) during day 1. Both patterns are plotted versus the ankle joint kinematic pattern during the last minute of baseline walking. Pearson product moment correlation common variances (r^2) provide a quantitative measure of similarity in joint kinematic patterns (Derrick et al., 1994).

We used repeated measure ANOVAs to test for differences in normalized EMG RMS, joint angle correlation common variances, and positive and negative exoskeleton work between days and condition (baseline minute 10, powered walking minute 1, 15 and 30, and post-adaptation minute 1 and 15). We set the significance level at $p<0.05$ and used Tukey honestly significant difference (THSD) post hoc tests.

To test for differences in motor adaptation rate during powered and post-adaptation walking, we calculated time to steady state for soleus stance RMS EMG, ankle joint correlation, and exoskeleton positive and negative mechanical work. We defined an envelope of steady-state behavior during powered walking based on the mean ± 2 SD (Noble and Prentice, 2006) of the final 15 min of day 2. Linear regression of data in this period revealed slopes that were not statistically different from zero ($p>0.05$). Time to steady state during powered walking was calculated as the time until values entered the envelope for at least three consecutive minutes and did not have any two consecutive minutes outside the envelope afterwards. For post-adaptation walking, similar methods were used but the steady-state envelope was determined as the mean ± 2 SD of data from 10 min of non-powered walking (the last 5 min of both baseline and post-adaptation walking) on day 2. Linear regression of the data in these periods also revealed slopes that were not statistically different from zero ($p>0.05$).

To make an estimate of the amount of assistance that the powered exoskeleton provided during walking, subjects returned for a third testing session of over ground walking. We recorded kinematic and force platform data during normal over ground walking at 1.25 m/s without wearing the exoskeleton. We calculated net torques and work performed about the ankle joint using commercial software (Visual3D, C-Motion Inc.) to perform inverse dynamic calculations. Lower limb inertial properties were estimated based on anthropometric measurements of the subjects (Zatsiorsky, 2002).

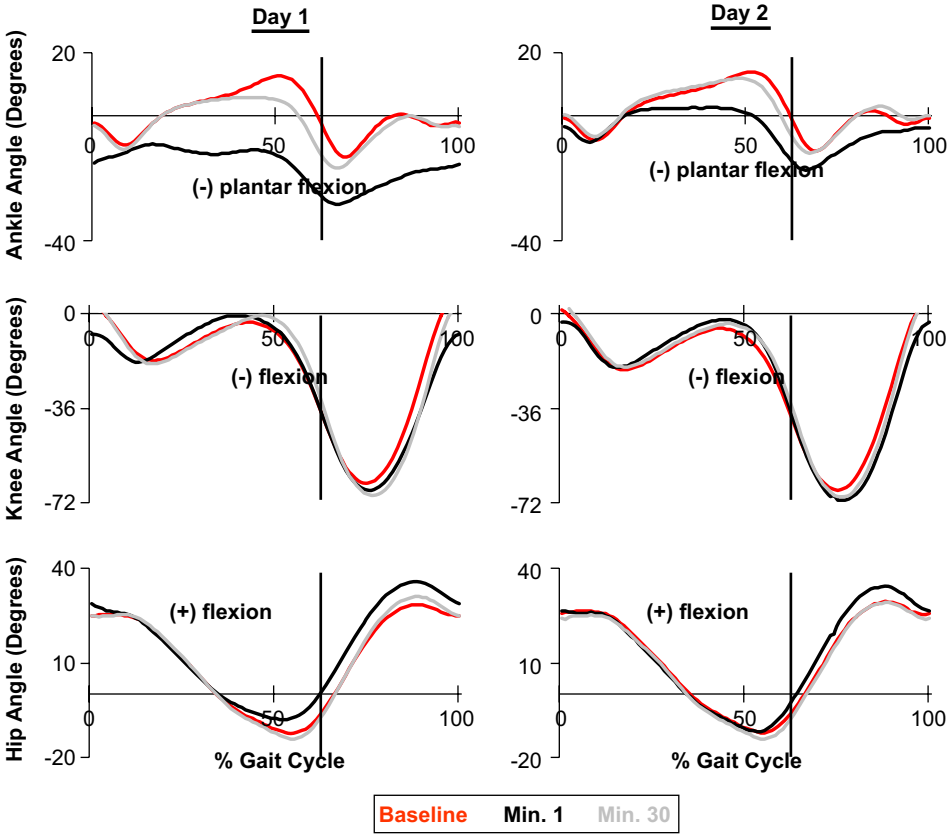

Fig. 3. Joint kinematic patterns. Ankle, knee and hip movement patterns are shown for the last minute of baseline walking (baseline, red line), the first minute of powered walking (minute 1, black line), and the last minute of powered walking (minute 30, grey line) during day 1 and day 2. Data are the average of all subjects. Vertical black lines represent the average toe-off time. The ankle kinematic pattern showed greatly increased plantar flexion throughout the stride cycle during the initial powered condition (day 1, minute 1). By the end of the second training session (day 2, minute 30), there were similar degrees of dorsiflexion and plantar flexion as the baseline pattern. The hip and knee kinematic patterns were similar across all testing conditions.

3. Results

3.1. Day 1, powered minute 1

When subjects first received additional plantar flexor torque from the powered exoskeleton, they demonstrated an immediate and substantial change in walking pattern (Fig. 3 and Movie 2 online supplement). Peak plantar flexion angle increased from $-13.3\pm3.6^\circ$ (mean $\pm$ SD) during baseline to $-28.3\pm9.1^\circ$ during the first minute of powered walking. The deviation in kinematics was reflected by a significant change in ankle angle correlation common variance compared to baseline (THSD, $p<0.05$) (Fig. 4). In addition, during the first minute of powered walking both knee and hip angle correlation common variance were significantly different from baseline (THSD, $p<0.05$). The angle correlation common variances during the first minute of powered walking (ankle 0.29 ± 0.2; knee 0.81 ± 0.1; hip 0.90 ± 0.1) were the lowest values observed during the 2 test days. While the changes in angle correlation common variance during the first minute of powered walking were significant at all three joints the magnitude of change at the ankle was nearly four-fold that of the knee or hip.

Subjects had a relatively continuous soleus activation pattern throughout stance during minute 1 (Fig. 5). As a result of the soleus recruitment pattern, the exoskeleton produced plantar flexor torque throughout stance (Fig. 6). This yielded negative exoskeleton mechanical power early in stance and positive exoskeleton mechanical power late in stance (Fig. 6).

Many other muscles also demonstrated increased activation during the first minute of powered walking (Fig. 7). Tibialis anterior, medial gastrocnemius, lateral gastrocnemius, vastus medialis, vastual lateralis, rectus femoris, and medial hamstrings all had significantly greater EMG RMS at minute one compared to baseline (THSD, $p<0.05$).

3.2. Day 1, powered minute 30

With practice walking with the powered exoskeleton, ankle kinematics became similar to normal (Movie 3 online supplement). At powered minute 30, ankle angle correlation common variance had increased significantly (0.64 ± 0.11) compared to minute 1 (THSD, $p<0.05$). However, ankle angle correlation common variance was still significantly different from baseline after 30 min of walking (THSD, $p<0.05$). The adaptation period of ankle angle correlation common variance was 23.8 ± 9.8 min (Fig. 8). After 30 min of practice, knee correlation common variance was still significantly different from baseline but had increased significantly from minute 1 to 0.91 ± 0.04 (THSD, $p<0.05$). Hip angle correlation common variance was not significantly different from baseline at minute 15 or 30.

The timing of soleus activation returned to a bursting pattern similar to baseline with practice, although the amplitude substantially decreased (Fig. 5). Soleus stance EMG RMS was different from baseline at powered minutes 1, 15, and 30 (THSD, $p<0.05$). The soleus stance RMS adaptation period during the 30 min of powered walking on day 1 was 23.8 ± 8.8 min (Fig. 8). EMG RMS in all other muscles during minutes 15 and 30 of powered walking was not significantly different from baseline (THSD, $p>0.05$). There were no significant differences in positive work between minutes 1, 15, and 30 of powered walking (THSD, $p>0.05$) (Fig. 9). Negative work significantly decreased from minute 1 to minute 30 (THSD, $p<0.05$) (Fig. 9).

3.3. Day 1, post-adaptation

When exoskeleton power was removed, subjects rapidly returned to ankle kinematics and soleus activation patterns

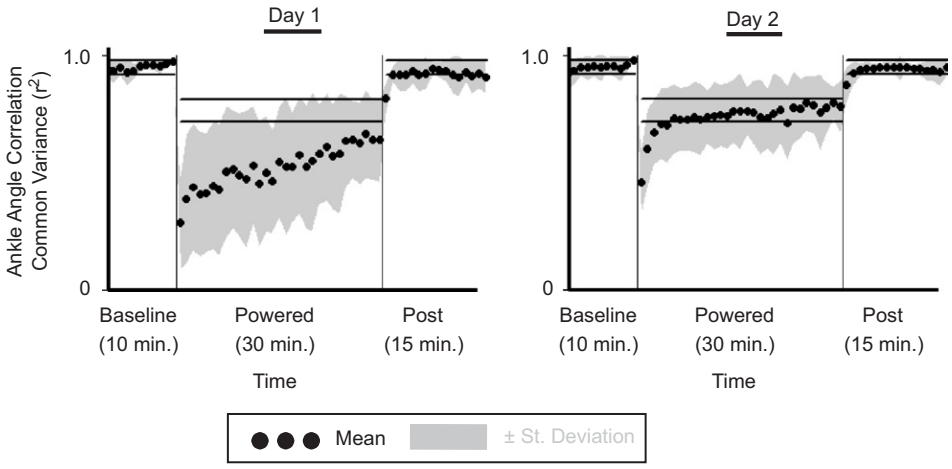

Fig. 4. Ankle joint kinematic correlation common variances. Mean data (black dots) $\pm$ 1 standard deviation (grey area) of all subjects ($n=10$) are shown for each minute. During powered conditions the horizontal black lines are the mean $\pm$ 2 standard deviations of group mean data from the last 15 min of day 2, representing steady state dynamics. During baseline and post-adaptation conditions horizontal black lines are the mean $\pm$ 2 SD of group mean data from the last 5 min of baseline and post-adaptation during day 2. The steady state envelopes displayed are calculated for the group mean data for display purposes only, individual subject analyses were used for statistical tests.

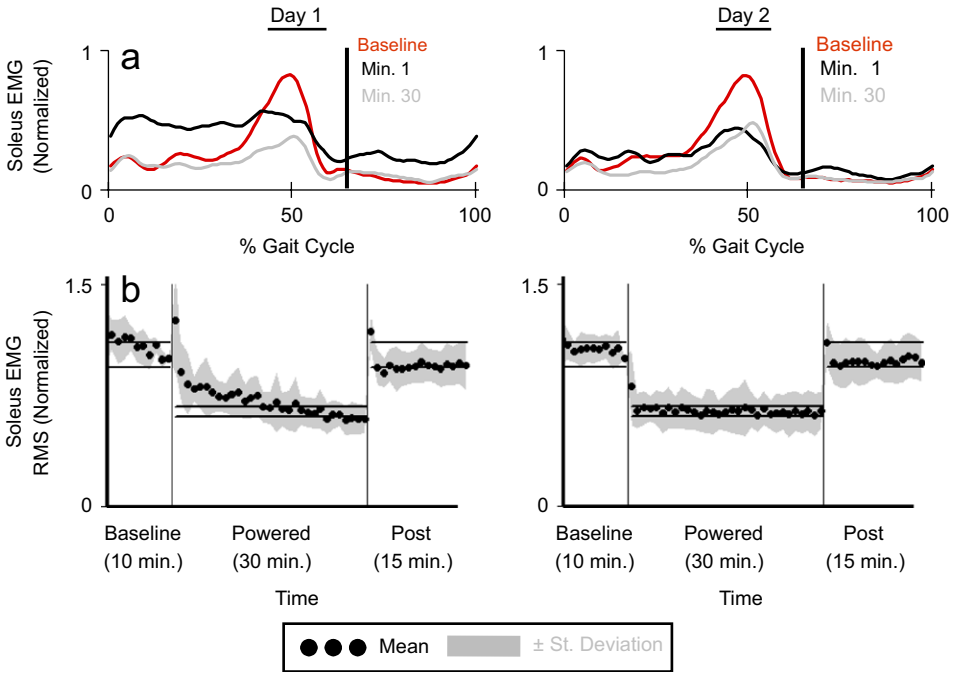

Fig. 5. (a) Soleus muscle activity patterns averaged across all subjects. During initial walking with the powered exoskeleton (day 1, minute 1, black line), soleus EMG showed high tonic muscle activation. By the end of powered walking on the first day (day 1, minute 30, grey line), the soleus muscle activity pattern was similar to the pattern during baseline walking (baseline, red dashed line) but with reduced amplitude. EMG was rectified, averaged, and low-pass filtered with a zero lag Butterworth filter (cutoff frequency 10 Hz). Vertical black lines represent average toe-off time. (b) Soleus EMG RMS amplitudes during stance. Mean data (black dots) ± 1 SD (grey area) of all subjects ($n = 10$) are shown for each minute. During powered conditions the horizontal black lines are the mean ± 2 standard deviations of group mean data from the last 15 min of day 2, representing steady-state dynamics. During baseline and post-adaptation conditions horizontal black lines are the mean ± 2 SD of group mean data from the last 5 min of baseline and post-adaptation during day 2. The steady-state envelopes displayed are calculated for the group mean data for display purposes only, individual subject analyses were used for statistical tests.

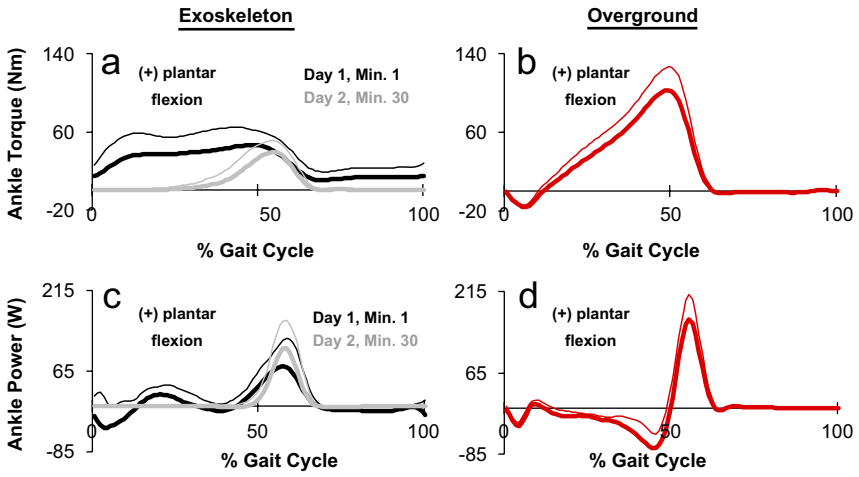

Fig. 6. (a) Exoskeleton mechanical torque during the gait cycle for powered walking on day 1, minute 1 (black line) and day 2, minute 30 (grey line). These data represents only the portion of the total ankle torque produced by the exoskeleton. Data are averaged from all subjects. (b) Average ankle torque calculated from inverse dynamics during normal overground walking with no exoskeleton. (c) Average plantar flexor power provided by the exoskeleton during the gait cycle for powered exoskeleton walking on the first day, first minute (black line) and the second day, 30th minute (grey line). These data represent only the portion of the total ankle power produced by the exoskeleton. Data are averaged from all subjects. Negative values indicate the exoskeleton is absorbing energy, positive values indicate that the exoskeleton is producing energy. (d) Average ankle power calculated from inverse dynamics during normal overground walking with no exoskeleton. Bold lines represent mean data. Thin lines represent +1 SD.

similar to baseline (Figs. 4 and 5). Ankle, knee and hip angle correlation common variance during the first minute of post-adaptation walking was not significantly different from baseline (THSD, $p > 0.05$). Soleus EMG RMS during the first minute of post-adaptation was also not significantly different from baseline (THSD, $p > 0.05$).

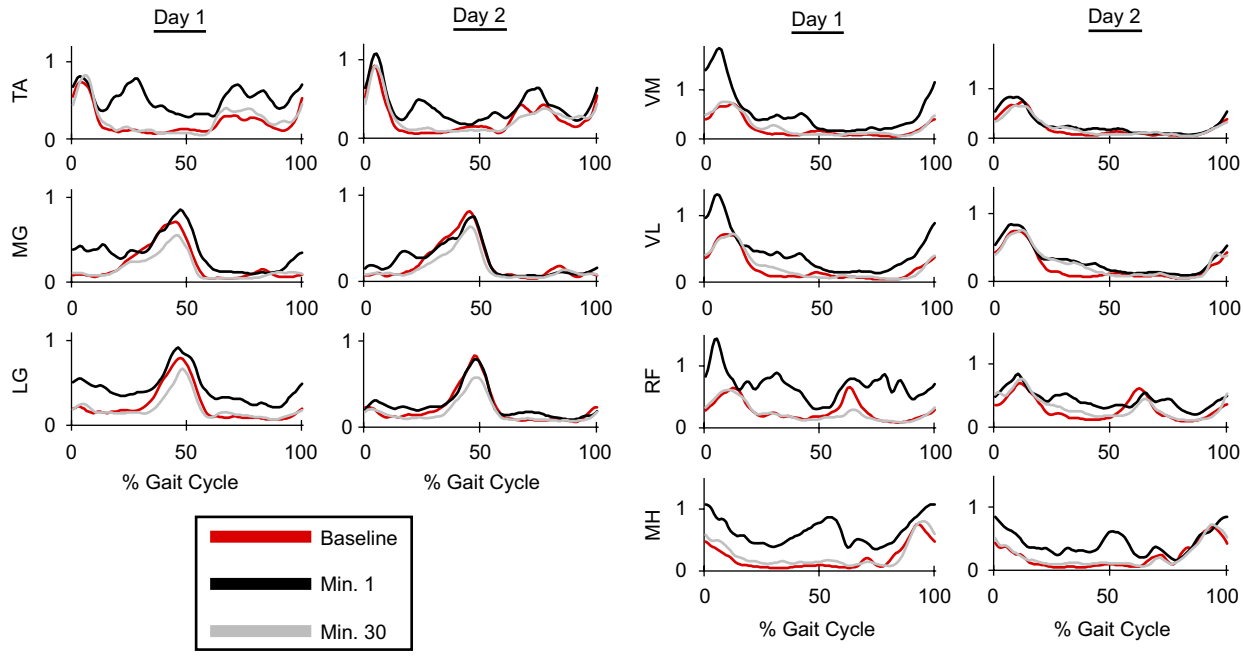

Fig. 7. Lower limb EMG patterns. Tibialis anterior (TA), medial gastrocnemius (MG), lateral gastrocnemius (LG), vastus medialis (VM), vastus lateralis (VL), rectus femoris (RF) and medial hamstring (MH) electromyography profiles during days 1 and 2. Data are averaged for all subjects (between 5 and 10 subjects per muscle due to missing data). All muscles were similar to baseline walking (baseline, red) by the end of the first training session. Medial gastrocnemius and lateral gastrocnemius patterns were slightly reduced in amplitude. Calculation of time to steady state for stance EMG RMS amplitudes of the other lower limb muscles revealed that all other muscles reached steady state before the soleus.

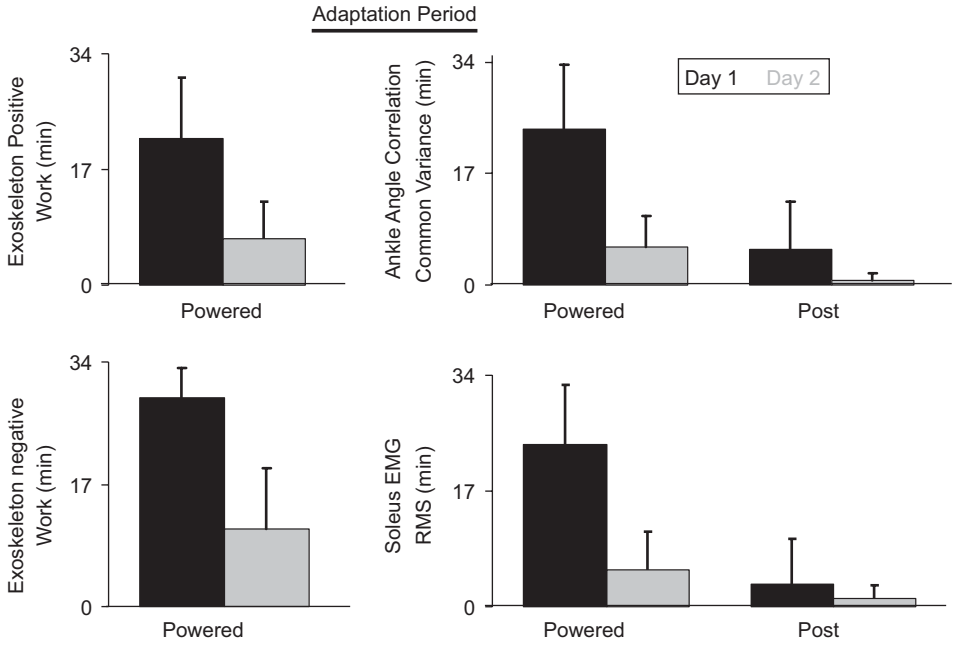

Fig. 8. Adaptation periods for day 1 (black) and day 2 (grey) during both powered and post-adaptation conditions. Data represent mean + SD for all 10 subjects.

3.4. Day 2, powered minute 1

During the first minute of powered walking on day 2, subjects' ankle kinematics were more plantar flexed throughout the gait cycle compared to baseline but not to the extent seen on day 1 (Fig. 3). Peak plantar flexion angle at minute 1 was $-17.4 \pm 8.1^{\circ}$. The ankle angle correlation common variance during the first minute of powered walking on day 2 was 0.46 ± 0.18 (Fig. 4). This common variance was significantly different from baseline walking on day 2 (THSD, $p < 0.05$) and from the first minute of powered walking on day 1 (THSD, $p < 0.05$), but it was not

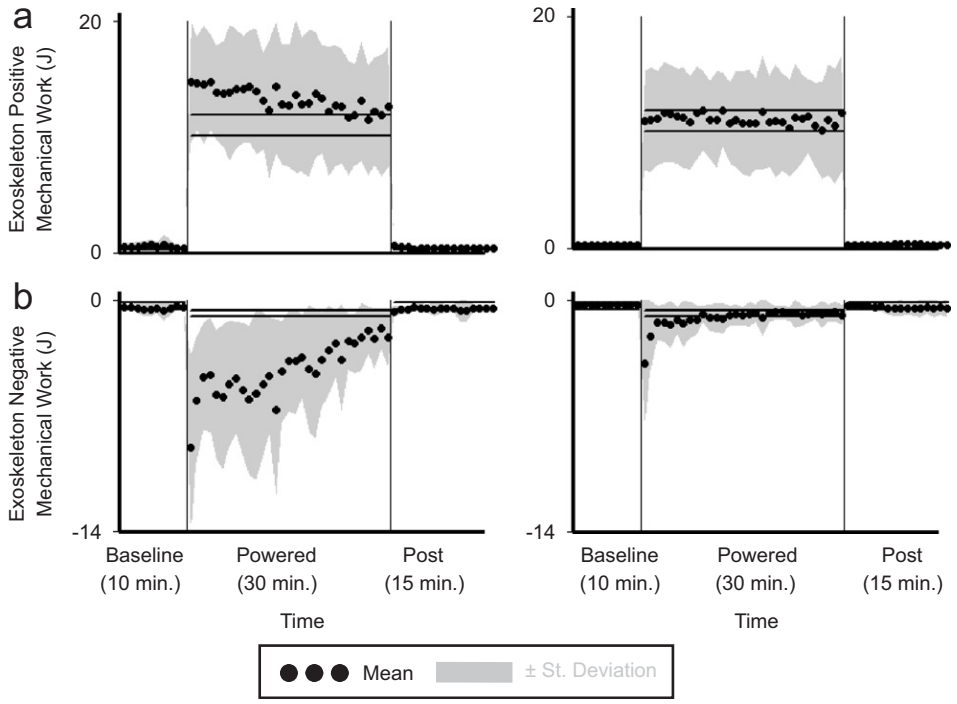

Fig. 9. Exoskeleton positive and negative mechanical work. Mean data (black dots) ± 1 SD (grey area) of all subjects ($n = 10$) are shown for each minute. During powered conditions the horizontal black lines are the mean ± 2 SD of group mean data from the last 15 min of day 2, representing steady-state dynamics. During baseline and post-adaptation conditions horizontal black lines are the mean ± 2 SD of group mean data from the last 5 min of baseline and post-adaptation during day 2. The steady-state envelopes displayed are calculated for the group mean data for display purposes only, individual subject analyses were used for statistical tests.

significantly different from minute 30 on day 1 (THSD, $p > 0.05$). Similarly, both knee and hip angle common variance were significantly different from baseline during minute 1 of powered walking on day 2 (THSD, $p > 0.05$).

Soleus activation displayed a clear bursting pattern during the first minute, similar to baseline but with decreased amplitude (Fig. 5). Soleus EMG RMS during minute 1 on day 2 was significantly less than minute 1 on day 1 (THSD, $p < 0.05$), but not different from minute 30 on day 1 (THSD, $p < 0.05$). There were no significant differences in exoskeleton positive mechanical work between minute 1 of day 2 and minute 1 of day 1 or minute 30 of day 1 (THSD, $p > 0.05$). During minute 1 of day 2, exoskeleton negative mechanical work was significantly less than during minute 1 of day 1 (THSD, $p < 0.05$) but not significantly different from minute 30 of day 1 (THSD, $p > 0.05$).

The only differences in EMG RMS in muscles other than soleus occurred in tibialis anterior and medial hamstrings, with significantly larger values during minute 1 compared to baseline (THSD, $p < 0.05$).

3.5. Day 2, powered minute 30

With practice on day 2, subjects walked with a similar ankle kinematic pattern to normal. At the end of 30 min of powered walking, subjects had significantly increased their ankle angle correlation common variance (0.78 ± 0.08) compared to powered minute 1 (THSD, $p < 0.05$) (Fig. 4). However, the common variance at minute 30 on day 2 was still significantly different from baseline (THSD, $p < 0.05$). The adaptation period on day 2 for the ankle angle correlation common variance was 5.8 ± 4.7 min. This adaptation period was significantly less than day 1 (ANOVA, $p < 0.0001$) (Fig. 8). By powered minute 30 on day 2 neither knee nor hip angle correlation common variance was significantly different from baseline (THSD, $p < 0.05$).

Soleus EMG RMS at minute 30 of powered walking was ($65 \pm 13\%$) significantly lower than baseline (THSD, $p < 0.05$). The adaptation period for soleus EMG RMS during powered walking on day 2 (5.5 ± 5.5 min) was significantly less than day 1 (ANOVA, $p < 0.0001$). The exoskeleton produced a peak positive mechanical power of 107 W at the end of day 2, about 65% of the positive ankle power during normal (i.e. no exoskeleton) walking (Fig. 6). There were no significant differences in exoskeleton positive or negative mechanical work between minutes 1, 15, and 30 on day 2 (THSD, $p > 0.05$). Exoskeleton positive and negative mechanical work were significantly less during day 2 than day 1 (ANOVA, $p < 0.05$). The adaptation periods for exoskeleton positive and negative mechanical work were significantly less on day 2 compared to day 1 (ANOVA, $p < 0.05$) (Fig. 8).

No other muscles had EMG RMS values significantly different from baseline during minutes 15 and 30 of powered walking on day 2 (THSD, $p > 0.05$).

3.6. Day 2, post-adaptation

On day 2, ankle kinematics and soleus muscle activation rapidly returned to baseline levels when exoskeleton power was removed. Ankle, knee and hip angle correlation common variance and soleus EMG RMS for the first minute of post-adaptation walking were not significantly different from baseline (THSD, $p>0.05$). The post-adaptation periods (Fig. 8) were not significantly different between days (ANOVA, $p>0.05$).

4. Discussion

The findings support our hypothesis that subjects would reduce soleus recruitment when walking with a powered exoskeleton providing supplemental plantar flexion torque proportional to soleus EMG. At the end of the second walking session, subjects walked with an ankle kinematic pattern significantly different from baseline. It is possible that further training would have resulted in additional modifications to muscle activation patterns and ankle kinematics. However, linear regression of data from the last 15 min on day 2 indicated all performance parameters had slopes not significantly different from zero. Therefore, further modifications would likely be relatively small and/or require much longer training periods.

The adaptation period observed on the first test day was relatively long (~24 min for ankle kinematics and soleus EMG) compared with previous studies investigating human locomotor adaptation to external perturbations (Ferris et al., 1999; Stephens and Yang, 1999; van Hedel et al., 2002; Emken and Reinkensmeyer, 2005; Lam et al., 2006). A difference between our study and previous research was that the perturbations in this study directly affected the relationship between muscle coordination and joint dynamics. Animal studies of locomotor adaptation to disrupted muscular coordination have found that considerable walking practice is required to be fully adapted (Lam and Pearson, 2002; Rossignol, 2006). In these studies the adaptation times required to reach steady state were on the order of days or weeks, not steps or minutes.

Although other studies have utilized exponential or power law fits of performance data to characterize motor adaptation, we did not find this approach helpful in our data analyses. Exponential and power law fits had r values lower than 0.2 for some individual subject data in our study. Recent modeling work suggests that there are at least two independent processes with different time scales underlying motor adaptation (Smith et al., 2006). Thus, a single adaptation rate from an exponential or power fit would not provide the best measure of motor adaptation rate. Using time to steady state (Noble and Prentice, 2006) as the measure of motor adaptation rate does not make any a priori assumptions about the shape of the motor adaptation data.

Results from our second day of testing demonstrated that subjects developed a lasting representation of limb dynamics when wearing the exoskeleton. Subjects learned and stored a new muscle activation pattern for locomotion. During minute 1 of day 2, soleus EMG and exoskeleton kinetics immediately returned to values similar to the final minute on day 1. A leading theory on the neural control of movement is that humans form predictive representations of system dynamics (i.e. internal model) when they experience modifications to their musculoskeletal mechanics or environment (Kawato and Wolpert, 1998; Davidson and Wolpert, 2005). Results from our study support the idea that humans form and store internal models of system dynamics for locomotion as evidenced by the improved performance on the second day of testing. Furthermore, our post-adaptation results indicate that humans can quickly return to their primary internal models when musculoskeletal mechanics are returned to normal.

The way subjects learned to use the exoskeleton provides insight into walking biomechanics. A simple model of bipedal walking suggests that the most energetically efficient method of powering walking is to input power from the ankle immediately before toe-off (Kuo, 2002). Subjects in our study adapted their motor patterns to use the powered exoskeleton in a similar manner. With practice, subjects increased peak positive power performed by the exoskeleton before toe-off and decreased negative work throughout the gait cycle. During the learning process, subjects initially activated many muscles almost continuously. With practice, they modified muscle activation to become more burst-like with clear on and off time periods. During the development of walking, children demonstrate similar muscle activation patterns, changing from almost continuous to burst activation (Okamoto and Goto, 1985; Thelen and Cooke, 1987; Bradley and Smith, 1988; Okamoto et al., 2003). Both observations suggest that humans learn when not to activate muscles during walking rather than learning when to activate them. Continuously activating muscles creates higher joint impedance and likely increases walking stability (Duan et al., 1997; van Soest et al., 2003). The trade-off is high metabolic cost resulting from greater muscle forces and competing positive and negative work.

This study used a robotic exoskeleton to investigate human locomotor adaptation. Subjects demonstrated a longer adaptation period in response to the imposed neuromuscular discoordination than has been demonstrated for environmental perturbations. However, with practice subjects learned to use the additional exoskeleton power effectively during walking. In addition subjects demonstrated an ability to store the learned exoskeleton motor program.

Acknowledgments

The authors thank Catherine Kinnaird and members of the Human Neuromechanics Laboratory for assistance in collecting and analyzing data. We also thank Ammanath Peethambaran, C.O., and the staff of the University of

Michigan Orthotics and Prosthetics Center for help with designing and fabricating parts of the exoskeleton. Supported by NIH R01 NS045486.

Appendix A. Supplementary data

Supplementary data associated with this article can be found in the online version at doi:10.1016/j.jbiomech.2006.07.025.

References

Bradley, N.S., Smith, J.L., 1988. Neuromuscular patterns of stereotypic hindlimb behaviors in the first two postnatal months. I. Stepping in normal kittens. Brain Research 466 (1), 37–52.

Davidson, P.R., Wolpert, D.M., 2005. Widespread access to predictive models in the motor system: a short review. Journal of Neural Engineering 2 (3), S313–S319.

Derrick, T.R., Bates, B.T., Dufek, J.S., 1994. Evaluation of time-series data sets using the Pearson product-moment correlation coefficient. Medicine and Science in Sports and Exercise 26 (7), 919–928.

Duan, X.H., Allen, R.H., Sun, J.Q., 1997. A stiffness-varying model of human gait. Medical Engineering and Physics 19 (6), 518–524.

Emken, J.L., Reinkensmeyer, D.J., 2005. Robot-enhanced motor learning: accelerating internal model formation during locomotion by transient dynamic amplification. IEEE Transactions on Neural Systems and Rehabilitation Engineering 13 (1), 33–39.

Farley, C.T., Houdijk, H.H., Van Strien, C., Louie, M., 1998. Mechanism of leg stiffness adjustment for hopping on surfaces of different stiffnesses. Journal of Applied Physiology 85 (3), 1044–1055.

Ferris, D.P., Czerniecki, J.M., Hannaford, B., 2005. An ankle-foot orthosis powered by artificial pneumatic muscles. Journal of Applied Biomechanics 21 (2), 189–197.

Ferris, D.P., Farley, C.T., 1997. Interaction of leg stiffness and surface stiffness during human hopping. Journal of Applied Physiology 82 (1), 15–22.

Ferris, D.P., Gordon, K.E., Sawicki, G.S., Peethambaran, A., 2006. An improved powered ankle-foot orthosis using proportional myoelectric control. Gait and Posture 23 (4), 425–428.

Ferris, D.P., Louie, M., Farley, C.T., 1998. Running in the real world: adjusting leg stiffness for different surfaces. Proceedings of the Royal Society of London: Biological Sciences 265 (1400), 989–994.

Ferris, D.P., Liang, K., Farley, C.T., 1999. Runners adjust leg stiffness for their first step on a new running surface. Journal of Biomechanics 32 (8), 787–794.

Gordon, K.E., Sawicki, G.S., Ferris, D.P., 2006. Mechanical performance of artificial pneumatic muscles to power an ankle-foot orthosis. Journal of Biomechanics 39 (10), 1832–1841.

Kawato, M., Wolpert, D., 1998. Internal models for motor control. Novartis Foundation Symposium 218 (1), 291–304 [discussion 304–7].

Kim, C.M., Eng, J.J., 2003. The relationship of lower-extremity muscle torque to locomotor performance in people with stroke. Physical Therapy 83 (1), 49–57.

Kim, C.M., Eng, J.J., Whittaker, M.W., 2004. Level walking and ambulatory capacity in persons with incomplete spinal cord injury: relationship with muscle strength. Spinal Cord 42 (3), 156–162.

Kuo, A.D., 2002. Energetics of actively powered locomotion using the simplest walking model. Journal of Biomechanical Engineering 124 (1), 113–120.

Lam, T., Anderschitz, M., Dietz, V., 2006. Contribution of feedback and feedforward strategies to locomotor adaptations. Journal of Neurophysiology 95 (2), 766–773.

Lam, T., Pearson, K.G., 2002. The role of proprioceptive feedback in the regulation and adaptation of locomotor activity. Advances in Experimental Medicine and Biology 508, 343–355.

Lay, A.N., Hass, C.J., Richard Nichols, T., Gregor, R.J., 2006. The effects of sloped surfaces on locomotion: an electromyographic analysis. Journal of Biomechanics, in press, doi:10.1016/j.jbiomech.2006.05.023.

Leroux, A., Fung, J., Barbeau, H., 1999. Adaptation of the walking pattern to uphill walking in normal and spinal-cord injured subjects. Experimental Brain Research 126 (3), 359–368.

Maclellan, M.J., Patla, A.E., 2006. Stepping over an obstacle on a compliant travel surface reveals adaptive and maladaptive changes in locomotion patterns. Experimental Brain Research 173 (3), 531–538.

Marigold, D.S., Patla, A.E., 2005. Adapting locomotion to different surface compliances: neuromuscular responses and changes in movement dynamics. Journal of Neurophysiology

Meinders, M., Gitter, A., Czerniecki, J.M., 1998. The role of ankle plantar flexor muscle work during walking. Scandinavian Journal of Rehabilitation Medicine 30 (1), 39–46.

Nadeau, S., Gravel, D., Arsenault, A.B., Bourbonnais, D., 1999. Plantarflexor weakness as a limiting factor of gait speed in stroke subjects and the compensating role of hip flexors. Clinical Biomechanics (Bristol, Avon) 14 (2), 125–135.

Noble, J.W., Prentice, S.D., 2006. Adaptation to unilateral change in lower limb mechanical properties during human walking. Experimental Brain Research 169 (4), 482–495.

Okamoto, T., Goto, Y., 1985. Human infant pre-independent and independent walking. In: Kondo, S. (Ed.), Primate Morphophysiology, Locomotor Analyses and Human Bipedalism. University of Tokyo Press, Tokyo, pp. 25–45.

Okamoto, T., Okamoto, K., Andrew, P.D., 2003. Electromyographic developmental changes in one individual from newborn stepping to mature walking. Gait and Posture 17 (1), 18–27.

Prentice, S.D., Hasler, E.N., Groves, J.J., Frank, J.S., 2004. Locomotor adaptations for changes in the slope of the walking surface. Gait and Posture 20 (3), 255–265.

Rossignol, S., 2006. Plasticity of connections underlying locomotor recovery after central and/or peripheral lesions in the adult mammals. Philosophical Transactions of the Royal Society of London Series B–Biological Science 361 (1473), 1647–1671.

Sawicki, G.S., Domingo, A., Ferris, D.P., 2006. The effects of powered ankle-foot orthoses on joint kinematics and muscle activation during walking in individuals with incomplete spinal cord injury. Journal of Neuroengineering Rehabilitation 3, 3.

Smith, M.A., Ghazizadeh, A., Shadmehr, R., 2006. Interacting adaptive processes with different timescales underlie short-term motor learning. PLoS Biology 4 (6), e179.

Stephens, M.J., Yang, J.F., 1999. Loading during the stance phase of walking in humans increases the extensor EMG amplitude but does not change the duration of the step cycle. Experimental Brain Research 124 (3), 363–370.

Thelen, E., Cooke, D.W., 1987. Relationship between newborn stepping and later walking: a new interpretation. Developmental Medicine and Child Neurology 29 (3), 380–393.

Tokuhiro, A., Nagashima, H., Takechi, H., 1985. Electromyographic kinesiology of lower extremity muscles during slope walking. Archives of Physical Medicine and Rehabilitation 66 (9), 610–613.

van Hedel, H.J., Biedermann, M., Erni, T., Dietz, V., 2002. Obstacle avoidance during human walking: transfer of motor skill from one leg to the other. Journal of Physiology 543 (Pt 2), 709–717.

van Soest, A.J., Haenen, W.P., Rozendaal, L.A., 2003. Stability of bipedal stance: the contribution of cocontraction and spindle feedback. Biological Cybernetics 88 (4), 293–301.

Zatsiorsky, V.M., 2002. Kinetics of Human Motion. Human Kinetics, Champaign, IL.